

# Chapter 7

## Review of Z-Source Solid-State Circuit Breakers



Keith A. Corzine and Robert W. Ashton

### 1 Introduction

The Z-source dc circuit breaker can be accurately categorized as a special type of solid-state circuit breaker (SSCB). Solid-state dc breakers were developed long ago, and over the years there has been considerable research into a wide variety of circuit designs [1–9]. Several recent publications sum up a few of these circuits [3–9]. The common principal of operation is to use a bi-directional semiconductor switch in the main path between the source and load. Next, a circuit is set up to quickly detect a fault, typically an over-current. The circuit then switches the semiconductor off to isolate the faulty load from the source. Naturally, the energy built up in the source inductance will create a large voltage across the semiconductor, and so an MOV can be placed across it to clamp the voltage until the current goes to zero [3–5]. Reference [3] discusses the testing of a prototype 1 kV 1 kA dual-pole bidirectional IGBT-based SSCB. Each bidirectional pole switch contains two series connected IGBTs with antiparallel diodes. A parallel connected MOV is utilized to passively limit the peak switch voltage. The breaker control employs a time-current curve which determines the variation in trip time versus the magnitude of the fault current. Two different source inductances are exploited to assess breaker performance: a low inductance for high  $di/dt$ , and a high inductance for energy absorption capability. This breaker was primarily studied in a power hardware in-the-loop simulation to emulate a future medium-voltage solid-state circuit breaker.

---

K. A. Corzine (✉)  
UC Santa Cruz, Santa Cruz, CA, USA  
e-mail: [corzine@ucsc.edu](mailto:corzine@ucsc.edu); [Keith@Corzine.net](mailto:Keith@Corzine.net)

R. W. Ashton  
Ashton Consulting, Thornton, PA, USA  
e-mail: [bob@ashtonconsultingllc.com](mailto:bob@ashtonconsultingllc.com)

© This is a U.S. government work and not under copyright protection in the U.S.; foreign copyright protection may apply 2023

I. C. Kizilyalli et al. (eds.), *Direct Current Fault Protection*, Power Systems,  
[https://doi.org/10.1007/978-3-031-26572-3\\_7](https://doi.org/10.1007/978-3-031-26572-3_7)

As discussed in [4], variations on the pole semiconductor switch design can include the parallel connection of reverse blocking IGCTs (RB-IGCTs) instead of series connected MOSFETs or IGBTs; this arrangement dramatically reduces on-state loss. In fact, the equivalent dual pole RB-IGCT-based breaker in [4] demonstrated a fivefold reduction in on-state power loss over equivalent series connected IGBTs. Further, this breaker's mechanical pole packages an MOV sandwiched between two hockey-puck type IGCTs. Orientation free pulsating heat pumps provide an excellent thermal path for both IGCTs and the MOV. The 1 kV 1.5 kA breaker has a voltage suppression index ( $VSI = V_{peak}/V_{bus}$ ) of 2.1 during fault clearing permitting the use of 2.5 kV RB-IGCTs. Other devices can be placed in parallel with the switch to contain peak switch voltage during a fault. One such example is a switched MOV. For [5] the electronic MOV is only connected during a fault through the use of an SCR and a passive breakover diode (BOD). Further, the BOD acts as a gate trigger and assists the MOV during standby by increasing its maximum continuous operating voltage. For the 2 kV 500A SSCB in [5], the peak fault switch voltage is only 2.84 kV easily allowing the use of 3.3 kV IGBTs. The series MOV with auxiliary SCR-BOD can reduce the transient over-voltage of the main switch by more than 30% (i.e., a VSI reduction from 2.2 [4] to 1.42 [5]).

A classical method of implementing a solid-state dc breaker is to add auxiliary resonant circuit [1] in parallel with the main switch that can be activated during a fault [2]. Upon detection of a fault, the resonant circuit is activated and the resonant current, opposing the main path current, forces the main switch current to zero. This concept has been expanded with recent developments including a main path switch with stacked SiC devices to reduce losses and wireless capacitive coupling of the resonant branch [6, 7]. In [7] the authors present three single-pole unidirectional dc breakers which utilize series-parallel switch combinations constructed in symmetrical layouts to optimize current sharing. The traditional MOV and resistor-capacitor-diode snubber circuits are optimized based on thermal dissipation and snubber charge time. The two 500 V class MOSFET breakers achieve a VSI of <2.26. The 2 kV class, 3-series 3-parallel, SiC breaker has a VSI of 2.44. The estimated efficiencies range from 99.94% to 99.96%. When extrapolated to a 2-pole bidirectional equivalent, the efficiency would be greater than 99.75%. The extrapolated efficiency of the baseline single element non-parallel control-breaker is approximately 99.5%.

Some variations on the SSCB involve power converter elements. An example is the T-breaker constructed from three branches of half-bridge modules [8]. The capacitors of the arm branches can be pre-charged using the center branch, and the breaker can readily use the charged capacitor as a clamping device rather than an MOV. The T-breaker is a fault protection device with modular multilevel converter functions that is capable of series and shunt compensation similar to a flexible ac transmission system (FACTS) device on a power system. The test results for the SiC-based 1 kV 500 A prototype T-breaker in [8] demonstrated the capability to successfully interrupt a 4.5 kA (nine times rated) fault current while minimizing submodule voltage to a VSI of 1.5. The full-current on-state efficiency was tested and found to be 99.58%. Another extensive scheme that employs the use of power

converters to limit fault current is realized with the iBreaker [9]. This topology involves back-to-back buck dc/dc converters with a shared inductor. It has the added advantage of controllable breaker behavior. The iBreaker includes a variable frequency PWM current limiting state for soft-start, fault authentication and fault locating functions. Two classes of GaN wide bandgap single-pole common ground iBreakers, made form series and parallel connected devices, were tested: a 380 V 20 A (1-series 5-parallel) and 1 kV 10 A (2-series 8-parallel). Each had an on-state efficiency of 99.5%.

The primary distinction of the Z-source breaker is that it does not rely on fault detection circuitry. Instead, an incipient fault takes a high-frequency path and causes the semiconductor current to trend towards zero as the fault current is increasing. After a very short time (microsecond scale) the semiconductor current goes to zero and can remove the fault. Therefore, one advantage of the Z-source breaker is not having to implement the fault detection circuitry. Another advantage is that breaker coordination is not needed in larger systems involving multiple breakers (either upstream or in parallel). This is because the Z-source breaker nearest to the fault will rapidly switch off. Further, the source current decreases when the fault occurs preventing other breakers from tripping, and also not subjecting the source to the fault current.

The Z-source breaker does have some limitations. Compared to other SSCBs, the Z-source breaker requires passive components which lead to increased volume and mass. The classic Z-source breaker can mistake large step changes in load for a fault. However, coupled-inductor versions can be tuned for fault sensitivity as described below. The Z-source breaker also does not naturally respond to long-term arcing faults. However, intelligent arc fault detection and switch-off capability can be added as shown below.

The review below will first discuss the origin of the Z-source breaker. Inspired by the Z-source inverter [10, 11] and impedance-source circuits [12–14], the Z-source solid-state dc circuit breaker was introduced [15–17]. Popular variations on the Z-source breaker will be discussed [18–29]. More practical and more significant variations involving coupled inductors are then reviewed [30–46]. Lastly, some Z-source breakers incorporated in power converters are considered [47, 48].

## 2 Z-Source Breaker Concept

The original Z-source inverter concept concatenates a crossed-impedance network with a standard six-transistor inverter [10, 11]. This circuit showed some unique characteristics such as interfacing with a voltage or current source as well as buck and boost operation. Over the years, the Z-source inverter has been researched heavily and has become a well-established circuit. Further, researchers have investigated a seemingly infinite number of impedance circuits [12–14]. As an example, a number of impedance circuits are shown in Fig. 7.1.

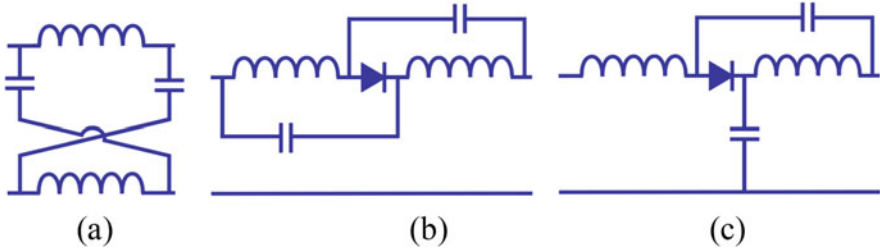
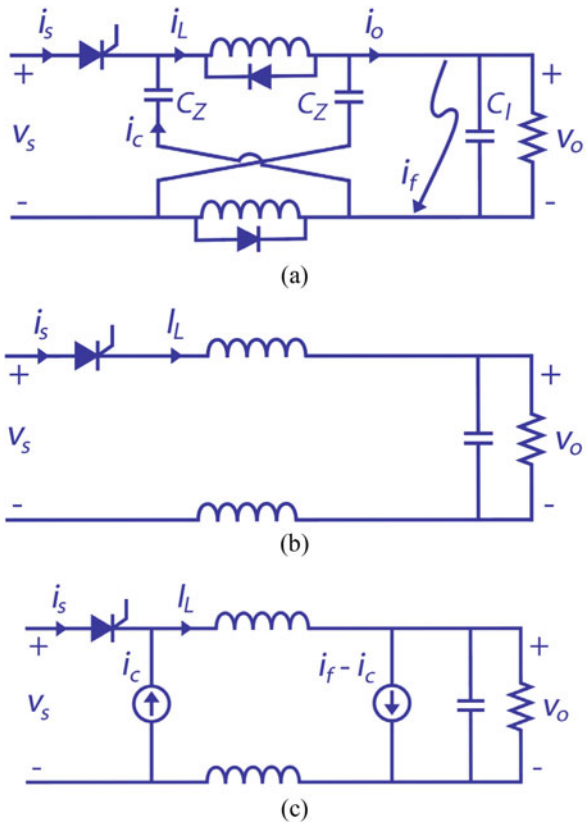


**Fig. 7.1** Examples of impedance-source networks: (a) crossed connection, (b) in-line connection, (c) capacitor-shunt connection

**Fig. 7.2** The Z-source dc circuit breaker: (a) classic design, (b) low-frequency equivalent circuit, (c) high-frequency equivalent circuit at fault inception



The Z-source circuit breaker combines the Z-source circuit with an SCR thyristor. The basic circuit is shown in Fig. 7.2 [15, 16]. As can be seen, this is the impedance-source circuit from Fig. 7.1a with an SCR on the front end. The operation of the circuit is as follows. During normal operation, the dc current takes the low-frequency path shown in Fig. 7.2b. When a sudden fault occurs, the transient current takes the high-frequency path through the capacitors. Effectively,

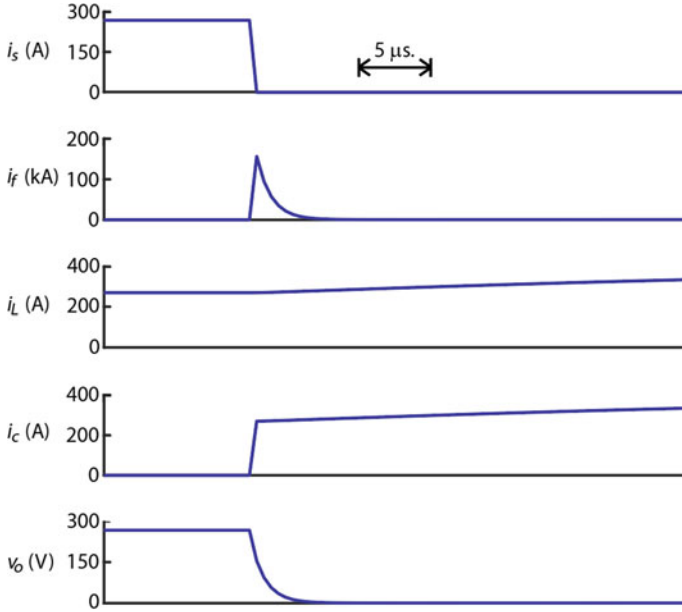


**Fig. 7.3** Waveforms of the classic Z-source circuit breaker

the transient current can be represented by the current sources shown in Fig. 7.2c. With the inductor current nearly constant, the transient capacitor current  $i_c$  pushes the SCR current to zero and, assuming the SCR is not gated, it switches off.

Figure 7.3 shows the waveforms of the Z-source breaker during a fault. These are labeled correspondingly to Fig. 7.2a. The important feature of a Z-source breaker, as originally conceived, is that as the fault current rises on the output of the breaker, the source current decreases. To be more exact, the source current is driven to zero by the capacitor current which is a function of the transient fault current according to (7.1). In this topology, the source current is the SCR current, and so, in a very rapid manner, the SCR will switch off and disconnect the faulty load from the source.

$$i_c = \left( \frac{C_Z}{C_Z + 2C_1} \right) i_f \tag{7.1}$$

After the breaking operation, there is a resonance formed by the inductors and capacitors in the breaker which is stopped by the diodes placed across the inductors at which point the capacitor current goes to zero. After this, the inductor current is extinguished in milliseconds due to the power loss of the diodes.

In comparison to other solid-state circuit breakers, the Z-source breaker has an additional burden in that added passive components are needed which increases the volume and mass. Furthermore, there is a requirement of an inverter grade SCR (or fast switch) with a small turn-off time [16]. Another disadvantage is that the

Z-source breaker is not set up for long time arcing faults. However, the circuit can be modified with an auxiliary switch and arc detection circuitry as well be shown below. The classic Z-source breaker may also misconstrue a large step in load as a fault. Newer designs, described herein, are tunable so that they can handle large step changes in load.

The Z-source breaker has a number of advantages and unique features when compared to other solid-state breakers. As demonstrated in Fig. 7.3, the response to a fault is automatic, without requiring external detection and control circuitry. This yields a significant advantage in that the fault response is very rapid. Another advantage is that the source (as well as the SCR) does not experience the fault current. In fact, the source current will not go over the system rated current. Probably one of the strongest advantages is autonomous operation in a multi-breaker system. In systems involving multiple Z-source breakers, only the one nearest the fault will switch off [17].

### 3 Variations on the Z-Source Breaker

Although derived with alternate consideration, it seems nearly all Z-source breakers could stem from impedance source circuits [13, 14]. As an example, consider the impedance source circuit of Fig. 7.1b. By replacing the diode with an SCR, the circuit breaker topology of Fig. 7.4 is obtained [18–20]. This variation with passive components in-line, sometimes called the parallel Z-source breaker [19, 20], has the feature that the source and load have the same common ground. One disadvantage of this circuit, as seen in the waveforms in Fig. 7.5, is that the source does experience a transient surge during the fault. Although the SCR current switches off immediately, the source current briefly goes to twice the steady-state value and then resonates a bit higher until the diodes stop the resonance.

Another variation of the Z-source breaker is the topology shown in Fig. 7.6 [21–23], sometimes referred to as a series Z-source breaker [21]. This topology can also be derived from the impedance-source circuits by comparing Fig. 7.6 to Fig. 7.1c. In this structure, the source and load have a common ground, which is expected in some power systems. A further technical detail is that the voltage transfer characteristic of this circuit is that of a low-pass filter. In contrast, the classic Z-source breaker

**Fig. 7.4** The Z-source breaker with in-line components

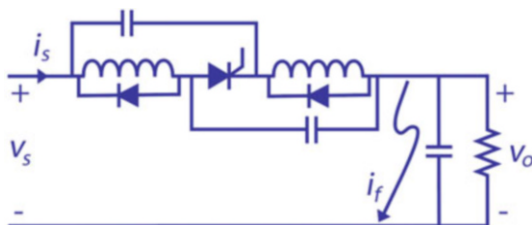




Fig. 7.5 Waveforms of the “parallel” Z-source breaker with in-line components

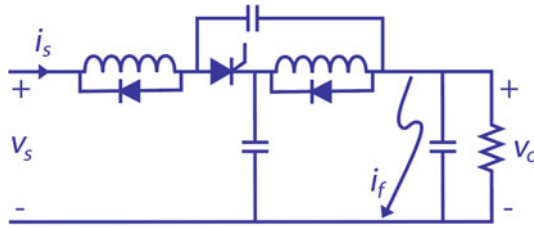


Fig. 7.6 The “series” Z-source breaker topology



Fig. 7.7 Waveforms of the “series” Z-source breaker topology

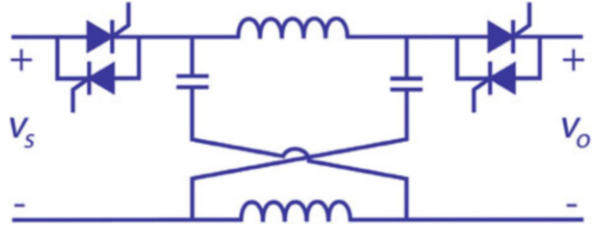
will attenuate high frequencies but has a resonant point based on the L-C values. In many dc power systems, the low-pass characteristic is desirable.

Figure 7.7 shows the waveforms of the series Z-source breaker. One drawback of this topology is that there is a series L-C impedance connecting the source and load after the SCR switches off. This causes the source to experience the resonant current after the fault. Although not as large as the fault current, there is an uptick in current drawn from the source when a fault occurs as can be seen in Fig. 7.7.

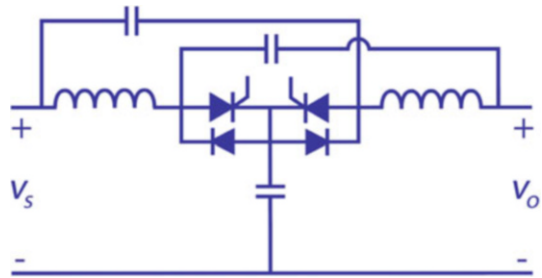
A number of other variations on the Z-source breaker have been conceived over the years besides those mentioned above. Most notably, a number of researchers have suggested bi-directional topologies where power flow can occur in both directions [25–29]. Dc power systems may require bidirectionality to permit energy flow between various dynamic sources and loads, especially in modern-day microgrids where loads may also generate power, such as battery energy storage systems.

Figure 7.8 shows a version of the Z-source breaker which is a straightforward extension of the classic Z-source breakers with bi-directional switches on each side

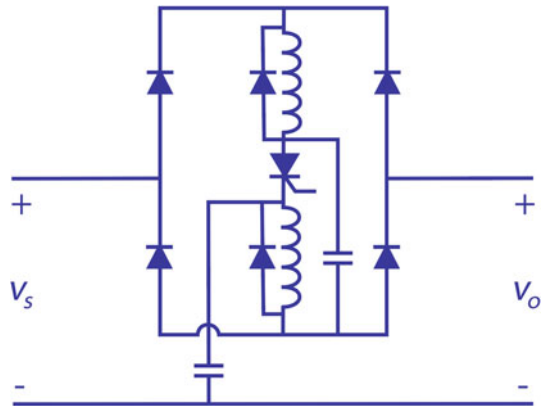
**Fig. 7.8** A Z-source circuit breaker adopted for bi-directional operation



**Fig. 7.9** Bi-directional Z-source breaker with in-line and shunt capacitors



**Fig. 7.10** Bi-directional Z-source breaker using a diode bridge



[25–27]. Once current is flowing in either direction, the gate signals can be removed to arm the breaker. The operation can be understood to be similar to that shown in Fig. 7.3.

Figure 7.9 shows another bi-directional variation of the Z-source breaker. The operation of this can be seen as similar to that of the breaker shown in Fig. 7.6 [27, 28]. On consideration of the circuit, it can be seen that this operation occurs with power flow in both directions.

Another bi-directional Z-source dc breaker is shown in Fig. 7.10 [29]. The four additional diodes connected to the source and load side act as a bridge rectifier. Thus, the current in the center branch will be unidirectional regardless of the overall power flow direction. Inside the bridge, the Z-source circuit operates much like that of Fig. 7.6.

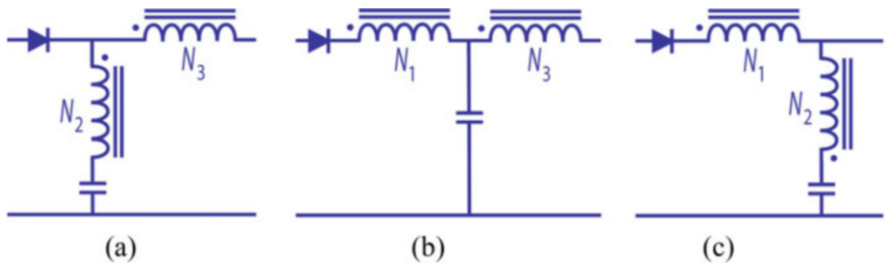
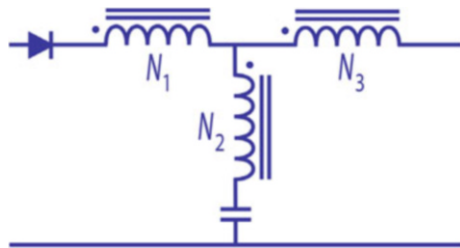


### 4 Coupled-Inductor Z-Source Breakers

In Z-source breaker circuits, coupling of the inductors yields considerable advantages. Namely, the circuit can be reconfigured and one of the capacitors can be eliminated. This was first pointed out in [30]. As with the circuits mentioned above, Z-source breakers with coupled inductors [30–46] can be derived from the general impedance-source circuits [12, 14]. Figure 7.11 shows a general magnetically coupled impedance-source circuit [14]. Some popular variations are shown in Fig. 7.12.

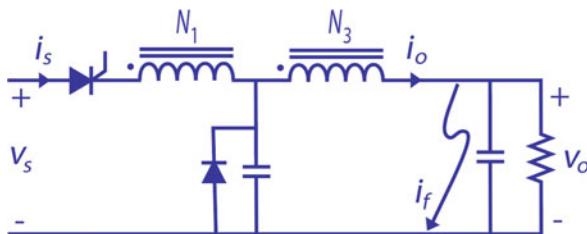
First, consider the T-source dc circuit breaker [30–36] shown in Fig. 7.13. This is a clear implementation of the circuit of Fig. 7.12b with the diode replaced by an SCR. A diode is placed in anti-parallel to the capacitor which will prevent the capacitor voltage from going negative and stops the resonance after the breaker has opened. This also exemplifies another advantage of coupled-inductor Z-source

**Fig. 7.11** The general magnetically coupled impedance-source circuit



**Fig. 7.12** Variations on the magnetically coupled impedance-source circuit: (a) the  $\Gamma$ -Z source network, (b) the T-source network, (c) the flipped  $\Gamma$  source network

**Fig. 7.13** The T-source dc circuit breaker



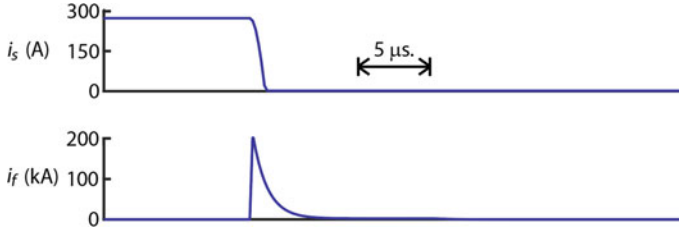


**Fig. 7.14** Waveforms of the T-source dc circuit breaker

breakers over uncoupled versions in that only one diode is required. (An alternative version places the diode across one of the coupled inductors [39]).

The T-source breaker works in the following way. During normal operation, the source supplies the load through the series combination of the primary and secondary inductor windings and the SCR; the breaker capacitor is charged to the source voltage. A fault at the output causes a current to circulate in the short path involving the capacitor and secondary winding  $N_3$ . Transient current flowing into the dot terminal of the secondary causes current to flow towards the source on the primary, forcing the SCR current to zero. Figure 7.14 shows the source current and fault current for the T-source breaker.

The T-source breaker has considerable advantages over the uncoupled Z-source breaker other than requiring only one capacitor. Further, the source and load share a common ground which may be important in certain applications. The source current is the SCR current and so will trend toward zero as the fault current rises. Additionally, the voltage transfer function will filter out high-frequency noise in the dc system above a resonant frequency.

The T-source breaker has an even bigger advantage over the uncoupled Z-source breaker and that is that the performance is tunable by choosing a turns ratio between the primary and secondary windings. This allows the designer to decide how much of a step in output current would be considered a fault and how much might just be a natural load step. To simplify the analysis, consider that the coupled inductors do not have leakage inductance and that a step change in load current happens instantaneously. Let the steady-state current be  $I_{dc}$ . With a step change in load current  $\Delta I_o$ , the breaker output current is

$$i_o = I_{dc} + \Delta I_o \quad (7.2)$$

Then, the current at the input of the circuit breaker is

$$i_s = I_{dc} - \frac{N_3}{N_1} \Delta I_o \quad (7.3)$$

Now, assume that the step in load is 100%; that is to say,  $\Delta I_o = I_{dc}$ . If the turns ratio is 1:1, the input current will go to zero according to (7.3), and the breaker will

**Fig. 7.15** The  $\Gamma$  Z-source breaker with auxiliary components

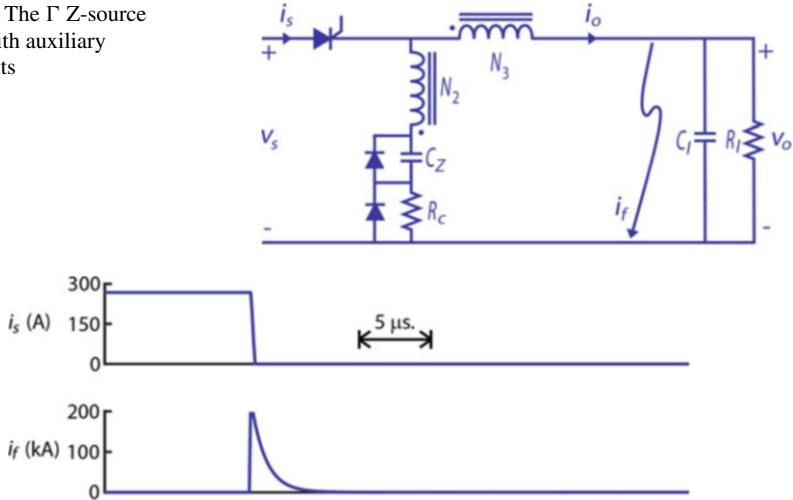


**Fig. 7.16** Performance of the  $\Gamma$  Z-source breaker during a fault

switch off. Therefore, load changes that are below 100% will not be treated as a fault, but a load change greater than 100% will appear as a fault. This behavior is not acceptable in some applications where loads are constantly switching on and off, microgrids, for example. In fact, uncoupled Z-source circuit breakers also have this property with the exception of some specific designs [22]. With the T-source breaker, the turns ratio can be set so that the breaker will not trip when there is a large change in load (i.e., 100%, 200%, 500%, etc.). However, a fault is typically well above these settings and will still trip the T-source breaker. Another interesting application for coupled-inductor breakers is where one might want the breaker to switch off when there is a 50% step change in load (just slightly above steady-state current). This would not trip a traditional Z-source breaker, but in the coupled-inductor breaker the turns ratio could be set with  $N_3/N_1 > 1$  for that to occur.

Using the circuit of Fig. 7.12a, another variation of the coupled-inductor Z-source breaker is formed: the  $\Gamma$  Z-source breaker [37]. An example is shown in Fig. 7.15. Therein, an added feature is introduced and that is the “soft-start” circuit. When the SCR is initially gated on, the capacitor  $C_Z$  will be charged through the charging resistor  $R_C$ . However, during a fault, the discharge path uses the diode in parallel with  $R_C$ . This feature can also be added to the T-source breaker described above.

Figure 7.16 shows the source current and fault current of the  $\Gamma$  Z-source breaker in response to a fault. As with the T-source breaker, the source current immediately goes to zero at the fault inception and so the performance is very similar. Considering this in more detail, researchers have noted that the output current  $i_o$  spike will be less during a fault with the  $\Gamma$  Z-source breaker as compared to the T-source breaker [34].

**Fig. 7.17** The flipped  $\Gamma$  Z-source breaker with auxiliary components

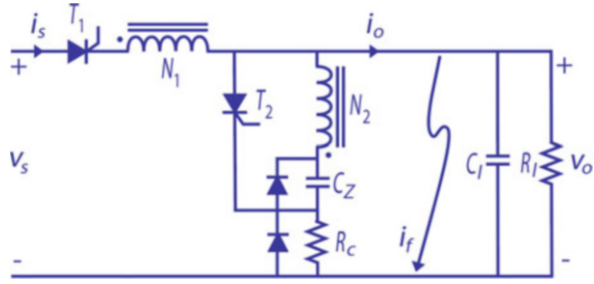


**Table 7.1** Parameters of the flipped  $\Gamma$  Z-source breaker example

$v_s = 270 \text{ V}$	$L_{m1} = 100 \text{ } \mu\text{H}$	$N_1/N_2 = 6$	$R_{l1} = 5 \text{ } \Omega$
$R_c = 10 \text{ } \Omega$	$C_Z = 100 \text{ } \mu\text{F}$	$C_1 = 0.1 \text{ mF}$	$R_{l2} = 1 \text{ } \Omega$

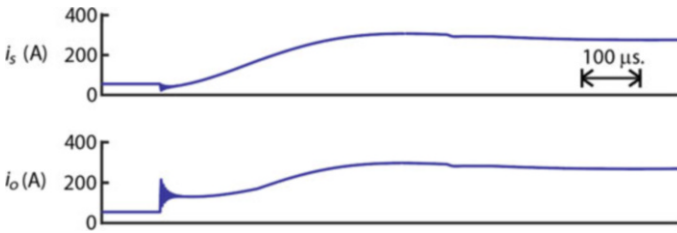


**Fig. 7.18** Performance of the flipped  $\Gamma$  Z-source breaker during a step in load

Following the circuit in Fig. 7.12c, an example of a flipped  $\Gamma$  coupled-inductor dc breaker [38–41] is shown in Fig. 7.17. Therein, another feature is introduced and that is the addition of a switch-off SCR  $T_2$ . If this SCR is activated in the steady-state, the capacitor  $C_Z$  discharges into the winding  $N_2$  causing  $T_1$  to switch off. Therefore,  $T_1$  and  $T_2$  can be used to switch the circuit on and off. This added switch introduces an important feature to the breaker. By monitoring the current  $i_o$ , long-term faults with low  $di/dt$  (such as arcing faults) can be detected and the breaker can be switched off via  $T_2$ . For the flipped  $\Gamma$  breaker, this has been demonstrated where an arcing fault was identified using a short-time Fourier transform and a clustering algorithm [40]. This setup protects dc systems with both low  $di/dt$  and rapid-inception faults. As with the  $\Gamma$  Z-source breaker, the flipped  $\Gamma$  Z-source breaker has an advantage over the T-source breaker in that the steady-state current only flows in one winding which reduces steady-state power losses a bit.

To illustrate the operation with a numerical example, the system parameters shown in Table 7.1 are to be used. The two load resistance values represent a light load of  $5 \text{ } \Omega$  switching to a heavy load of  $1 \text{ } \Omega$ .

Figures 7.18 and 7.19 show two operating modes of the flipped  $\Gamma$  Z-source breaker. In Fig. 7.18, the circuit is initially operating in the steady-state with the source supplying power to the light load. The load is suddenly changed to the heavy load. From the parameters of Table 7.1, the load current will step from 54 to 270 A



**Fig. 7.19** Performance of the flipped  $\Gamma$  Z-source breaker during a fault

**Fig. 7.20** Topology of the Y-source dc breaker

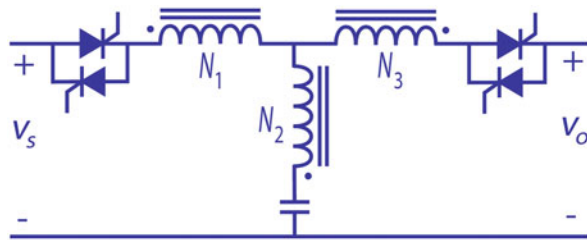
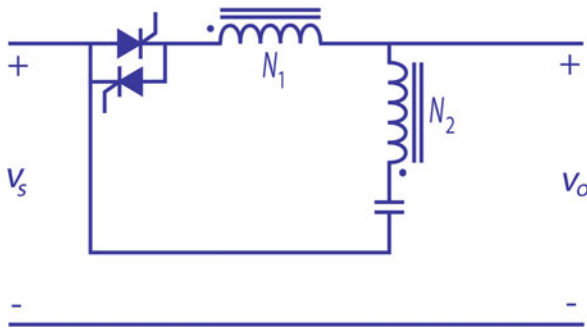


**Fig. 7.21** Topology of the O-Z-source dc breaker



during this change. According to (7.3), the step change in load will not switch off the SCR. The source current in Fig. 7.18 initially decreases as the load steps but not enough to switch the breaker off. Then, the source current then increases to match the output current.

Figure 7.19 shows the response of the flipped  $\Gamma$  Z-source breaker to a fault, where the SCR switches off. As with the T-source and classic Z-source breaker, the source current simply and rapidly goes to zero, starving the SCR of current and disconnecting the source from the fault.

There are a myriad of other types of Z-source breakers based on coupled inductors. An interesting type is the Y-source breaker [42, 43] which uses a three-winding transformer as shown in the fundamental circuit of Fig. 7.11 and is shown in Fig. 7.20. This type of breaker also has bi-directional capability. Other novel topologies such as the O-Z-Source breaker [44] of Fig. 7.21 and Q-Z-Source breaker [45] of Fig. 7.22 can be seen as derivatives of the flipped  $\Gamma$  and T-source breaker, respectively, with the capacitor connection attached to the positive terminal of the

**Fig. 7.22** Topology of the Q-Z-source dc breaker

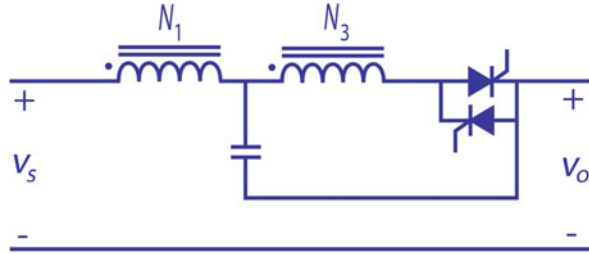
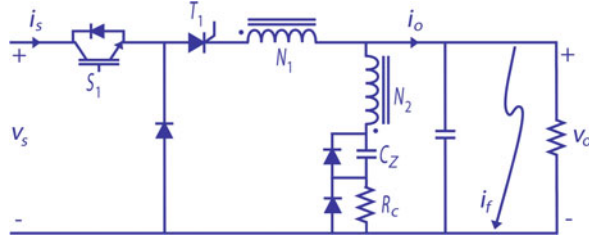


**Fig. 7.23** Integration of the Z-source breaker into a buck converter



load instead of the system ground. The capacitor connection of the T-source breaker can also be attached to the positive terminal of the source as another variation [46] which would look like a flipped version of the entire circuit of Fig. 7.22. Due to space limitations, these circuits are not described herein, but the interested reader is directed to the literature on coupled inductor breakers which have been growing in numbers in recent years [42–46].

## 5 Integrating Z-Source Breakers into Power Converters

The Z-source dc breaker has also been incorporated into dc/dc power converters. Two examples of this will be considered herein. First, Fig. 7.23 shows the flipped  $\Gamma$  Z-source breaker built into a standard buck dc/dc converter [47]. From the left, the typical buck converter switch  $S_1$  and freewheeling diode are seen. This is followed by the SCR  $T_1$  and components of the flipped  $\Gamma$  Z-source breaker. In this converter, the magnetizing inductance of the coupled inductor takes the place of the inductance in the buck converter. The output of the buck converter contains a capacitance as usual.

Table 7.2 shows the parameters used for a detailed simulation of the circuit of Fig. 7.23. In this example, a 270 V load is being supplied from a 600 V source, and so the duty cycle of the transistor switch is set accordingly. Figure 7.24 shows the simulation results. The source is supplying the load in steady-state when a fault occurs. From the inductor current, it appears the buck converter is in normal continuous conduction mode operation before the fault. This is the case except for the small perturbations in the secondary current that happen at the onset of the switch off state due to the leakage reactance of the coupled inductor and  $C_Z$ .

**Table 7.2** Parameters used in the dc/dc converter examples

$v_o = 270 \text{ V}$	$L_{m1} = 100 \text{ } \mu\text{H}$	$N_1/N_2 = 6$	$f_{sw} = 20 \text{ kHz}$
$R_c = 10 \text{ } \Omega$	$C_Z = 100 \text{ } \mu\text{F}$	$C_1 = 1 \text{ mF}$	$R_1 = 1 \text{ } \Omega$

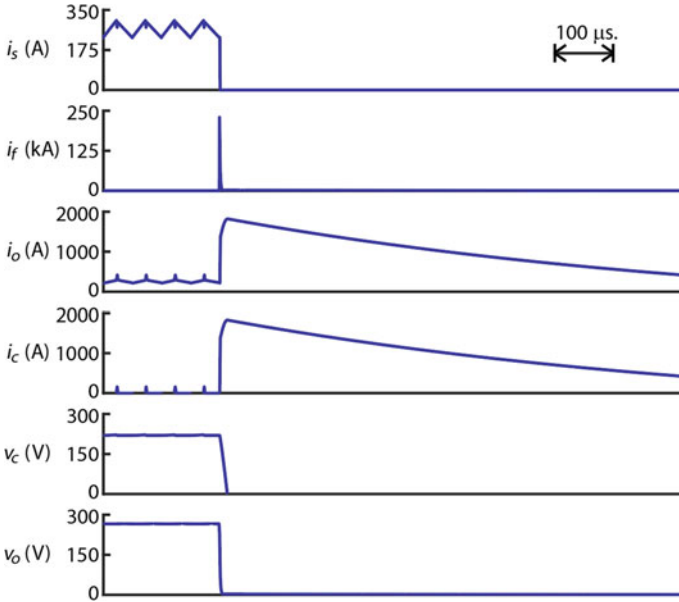
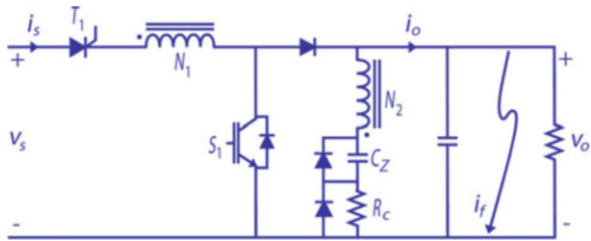


**Fig. 7.24** Performance of the buck converter with integrated Z-source breaker

**Fig. 7.25** Integration of the Z-source breaker into a boost converter



However, these can barely be seen in the source current waveform. When a fault occurs, the discharge of capacitor  $C_Z$  through the secondary winding  $N_2$  produces the expected result and the SCR switches off.

The next example is shown in Fig. 7.25. It is the flipped  $\Gamma$  Z-source breaker integrated into a standard boost dc/dc converter [48]. From the left, at the front end, the SCR is located in series with the primary winding of the transformer. As with the previous example, the magnetizing inductance of this transformer will be used as an energy conversion element in the converter. The transistor switch and freewheeling diode are seen in their expected configuration. The secondary winding is now located on the output of the boost converter.

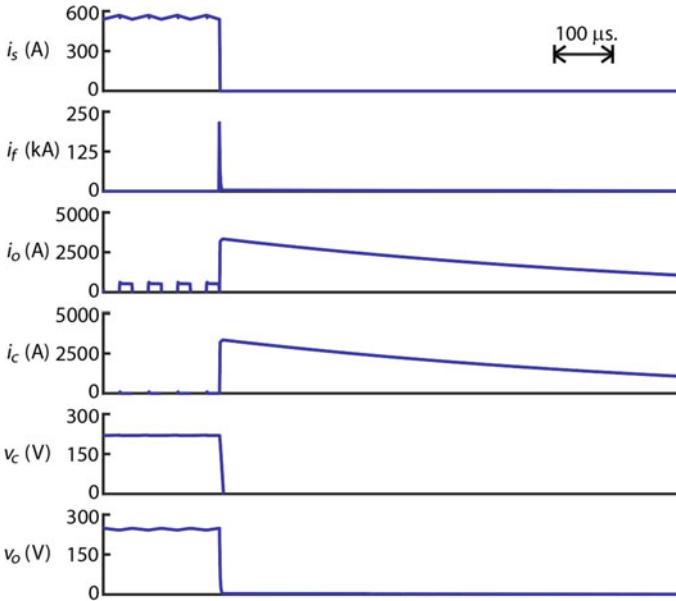


**Fig. 7.26** Performance of the boost converter with integrated Z-source breaker

The parameters in this example are shown in Table 7.2. In this case, a 120 V source supplies a 270 V load, and the boost converter duty cycle is set accordingly. Figure 7.26 shows the converter operation. When a fault occurs, the capacitor  $C_Z$  discharges through the secondary winding  $N_2$  causing a current which is reflected in the primary to switch the SCR off. The output current continues after the output voltage drops due to the magnetizing current of coupled inductors. However, this is extinguished quickly by the voltage drop across the diodes in parallel with  $R_C$  and  $C_Z$ .

## 6 Concluding Remarks

Like a traditional mechanical breaker, an SSCB is expected to respond to a fault and mitigate the affected circuit branch. This chapter first presented an overview of a number of dc SSCB arrangements. The many different SSCB configurations generally optimize one or more important attributes desired for a particular system. These attributes may include (1) cost, (2) time-current curve programmability, (3) functionality (i.e., multistate operation), (4) voltage and/or current suppression requirements, and (5) bidirectionality for energy flow between various dynamic sources and loads. The SSCB may be based on MOV protected semiconductor switches, more complex energy suppression MOVs and snubbers, or converter-



based multifunctional constructs. In general nearly all SSCB circuits rely on fault sensing and detection to actively open the main semiconductor switch path. However, the primary focus of this chapter is the Z-source breaker where fault sensing is not necessary, since passive pass-element commutation occurs “automatically” during a load fault transient. The Z-breaker concept began with the combination of the “zigzag” Z-source circuit in conjunction with a source-side SCR. This implies for most variations that the source current actually decreases as fault current rises. A number of variations of the Z-breaker concept are presented along with perceived advantages and disadvantages. For instance, the series and parallel Z-source breaker configurations have a common ground but unfortunately permit source transient current during a fault. However, a variety of coupled inductor arrangements do provide clear improvements over their uncoupled cousins: (1) common ground, (2) elimination of one capacitor and one diode, (3) tunable performance via the inductor turns ratio, and (4) high frequency filtering of the source. This chapter includes a coupled inductor Z-source breaker design example as well as suggestions on breaker system integration. Numerical examples of Z-source breakers integrated into buck and boost choppers are also presented.

## References

1. General Electric Company, *SCR Manual Including Triacs and Other Thyristors*, 5th edn. (1972)
2. M.J. Fisher, *Power Electronics* (PWS-Kent, 1991)
3. J. Langston, K. Schoder, M. Sloderbeck, M. Steurer, A. Rockhill, Testing operation and coordination of DC solid state circuit breakers, in IEEE Industrial Electronics Conference, pp. 3445–3452, October 2018
4. L. Qi, P. Cairoli, Z. Pan, C. Tschida, Z. Wang, V.R. Ramanan, L. Raciti, A. Antoniazzi, Solid-state circuit breaker protection for DC shipboard power systems: Breaker design, protection scheme, validation testing. *IEEE Trans. Ind. Appl.* **56**(2), 952–960 (2020)
5. L. Ravi, D. Zhang, D. Qin, Z. Zhang, Y. Xu, D. Dong, Electronic MOV-based voltage clamping circuit for DC solid-state circuit breaker applications. *IEEE Trans. Power Electron. Lett.* **37**(7), 7561–7565 (2022)
6. F. Lu, H. Zhang, R. Kheirollahi, Y. Wang, S. Zhao, A solid-state circuit breaker based on a wireless coupling and resonant circuit for MVDC systems. WIPO Patent WO2021211639A1, October 2021
7. S. Zhoa, R. Kheirollahi, Y. Wang, H. Zhang, F. Lu, Implementing symmetrical structure in MOV-RCD snubber-based DC solid-state circuit breakers. *IEEE Trans. Power Electron.* **37**(5), 6051 (2022)
8. Y. Zhang, X. Li, D. Ma, Y. Cong, F. Alsaif, Z. Zhang, R. Borjas, B. Hu, J. Wang, B. Riar, J. Ewanchuk, A. Sur, V. Blasko, Development of a 1 kV, 500 A, SiC-based T-type modular DC circuit breaker (T-breaker), in IEEE Workshop on Wide Bandgap Power Devices and Applications, November 2021
9. Y. Zhou, R. Na, Y. Feng, Z.J. Shen, GaN-based tri-mode intelligent solid-state circuit breakers for low-voltage DC power networks. *IEEE Trans. Power Electron.* **36**(6), 6596–6607 (2021)
10. F.Z. Peng, Z-source inverter, in IEEE Industry Applications Society Conference, vol. 2, pp. 775–781, October 2002
11. F.Z. Peng, Z-source inverter. *IEEE Trans. Ind. Appl.* **39**(2), 504–510 (2003)

12. F.Z. Peng, Z-source networks for power conversion, in IEEE Applied Power Electronics Conference, pp. 1258–1265, February 2008
13. Y.P. Siwakoti, F.Z. Peng, F. Blaabjerg, P.C. Loh, G.E. Town, Impedance-source networks for electric power conversion part I: A topological review. IEEE Trans. Power Electron. **30**(2), 699–716 (2015)
14. Y.P. Siwakoti, F. Blaabjerg, P.C. Loh, New magnetically coupled impedance (Z-) source networks. IEEE Trans. Power Electron. **31**(11), 7419–7435 (2016)
15. K.A. Corzine, R.W. Ashton, A new Z-source dc circuit breaker, in IEEE International Symposium on Industrial Electronics, Bari Italy, pp. 585–590, July 2010
16. K.A. Corzine, R.W. Ashton, A new Z-source dc circuit breaker. IEEE Trans. Power Electron. **27**(6), 2796–2804 (2012)
17. K.A. Corzine, Dc micro grid protection with the Z-source breaker, in IEEE Industrial Electronics Conference, Vienna Austria, November 2013
18. K.A. Corzine, R.W. Ashton, Structure and analysis of the Z-source MVDC breaker, in IEEE Electric Ship Technologies Symposium, Alexandria, VA, pp. 334–338, April 2011
19. P. Prempraneerach, M.G. Angle, J.L. Kirtley, G.E. Karniadakis, C. Chrysostomidis, Optimization of a Z-source DC circuit breaker, in IEEE Electric Ship Technologies Symposium, pp. 480–486, April 2013
20. T. Li, Y. Li, N. Liu, A new topological structure of Z-source DC circuit breaker. IEEE Trans. Circuits Syst. II Exp. Briefs **69**(7), 3294–3298 (2022)
21. A.H. Chang, B.R. Sennett, A. Avestruz, S.B. Leeb, J.L. Kirtley, Analysis and design of DC system protection using Z-source circuit breaker. IEEE Trans. Power Electron. **31**(2), 1036–1049 (2016)
22. A. Maqsood, A. Overstreet, K.A. Corzine, Modified Z-source dc circuit breaker topologies. IEEE Trans. Power Electron. **31**(10), 7394–7403 (2016)
23. V. Raghavendra I, S.N. Banavath, S. Thamballa, Modified Z-source DC circuit breaker with enhanced performance during commissioning and reclosing. IEEE Trans. Power Electron. **37**(1), 910–919 (2022)
24. A. Maqsood, K.A. Corzine, The Z-source breaker for fault protection in ship power systems, in IEEE International Symposium on Power Electronics, Electrical Drives, Automation and Motion, Ischia Island Italy, June 2014
25. A. Maqsood, K.A. Corzine, The Z-source breaker for ship power system protection, in IEEE Electric Ship Technologies Symposium, Alexandria, VA, June 2015
26. A. Maqsood, L. Li, K.A. Corzine, Low-voltage Dc testbed design for a Z-source breaker based protection scheme, in IEEE Clemson Power Systems Conference, Clemson SC, March 2016
27. D. Keshavarzi, T. Ghanbari, E. Farjah, A Z-source-based bidirectional DC circuit breaker with fault current limitation and interruption capabilities. IEEE Trans. Power Electron. **32**(9), 6813–6822 (2017)
28. S.G. Savaliya, B.G. Fernandes, Analysis and experimental validation of bidirectional Z-source DC circuit breakers. IEEE Trans. Ind. Electron. **67**(6), 4613–4622 (2020)
29. T. Bhaskar, S.L. Shaikh, A Z-source based bidirectional series circuit breaker for DC application, in IEEE International Conference on Smart Electronics and Communication, pp. 1283–1287, September 2020
30. A. Maqsood, K.A. Corzine, Z-source DC circuit breakers with coupled inductors, in IEEE Energy Conversion Congress and Exposition, September 2015
31. Y. Wang, W. Li, X. Wu, R. Xie, Z. Zhang, H. Wang, A novel solid-state circuit breaker for DC microgrid system, in IEEE International Conference on Electrical Systems for Aircraft, Railway, Ship Propulsion and Road Vehicles & International Transportation Electrification Conference, November 2018
32. C. Li, Z. Nie, H. Li, Y. Zhang, A novel solid-state protection scheme for DC system, in IEEE International Power Electronics and Motion Control Conference, pp. 2039–2042, May 2016
33. W. Song, N. An, Y. Wang, A novel bidirectional T-source DC circuit breaker for DC microgrids, in IEEE Conference on Industrial Electronics and Applications, pp. 1540–1545, June 2019

34. W. Li, Y. Wang, X. Wu, X. Zhang, A novel solid-state circuit breaker for on-board DC microgrid system. *IEEE Trans. Ind. Electron.* **66**(7), 5715–5723 (2019)
35. Y. Yang, C. Huang, A low-loss Z-source circuit breaker for LVDC systems. *IEEE J. Emerg. Sel. Top. Power Electron.* **9**(3), 2518–2528 (2021)
36. X. Diao, F. Liu, Y. Song, M. Xu, Y. Zhuang, W. Zhu, X. Zha, A new efficient bidirectional T-source circuit breaker for flexible DC distribution networks. *IEEE J. Emerg. Sel. Top. Power Electron.* **9**(6), 7056–7065 (2021)
37. Z. Zhou, J. Jiang, S. Ye, C. Liu, D. Zhang, A  $\Gamma$ -source circuit breaker for DC microgrid protection. *IEEE Trans. Ind. Electron.* **68**(3), 2310–2320 (2021)
38. K.A. Corzine, Circuit breaker for DC micro grids, in *IEEE International Conference on DC Microgrids*, June 2015
39. K.A. Corzine, A new coupled-inductor circuit breaker for DC applications. *IEEE Trans. Power Electron.* **32**(2), 1411–1418 (2017)
40. A. Maqsood, N. Rossi, Y. Ma, K.A. Corzine, L. Parsa, D. Oslebo, A coupled-inductor Dc breaker with STFT-based arc detection, in *IEEE Applied Power Electronics Conference*, New Orleans, LA, March 2020
41. H. Al-khafaf, J. Asumadu,  $\Gamma$ -Z-source DC circuit breaker operation with variable coupling coefficient  $k$ , in *IEEE International Conference on Electro Information Technology*, pp. 492–496, May 2017
42. H. Al-khafaf, J. Asumadu, Y-source bi-directional DC circuit breaker, in *International Power Electronics Conference (ECCE Asia)*, pp. 3445–3449, May 2018
43. Y. Wang, R. Dong, Z. Xu, Z. Kang, W. Yao, W. Li, A coupled-inductor-based bidirectional circuit breaker for DC microgrid. *IEEE J. Emerg. Sel. Top. Power Electron.* **9**(3), 2489–2499 (2021)
44. Z. Zhou, J. Jiang, S. Ye, D. Yang, J. Jiang, Novel bidirectional O-Z-source circuit breaker for DC microgrid protection. *IEEE Trans. Power Electron.* **36**(2), 1602–1613 (2021)
45. L. Yi, J. Moon, Bidirectional Q-Z-source DC circuit breaker. *IEEE Trans. Power Electron.* **37**(8), 9524–9538 (2022)
46. M. Marwaha, K. Satpathi, J. Pou, D.A. Molligoda, C. Gajanayake, A. Kumar Gupta, Coupled-inductor-based bidirectional Z-source breaker for DC system protection, in *IEEE Industrial Electronics Society Conference*, pp. 3433–3438, October 2020
47. J.Y.K. Chong, D.J. Ryan, H.D. Torresan, B. Bahrani, A buck converter with integrated circuit breaker, in *IEEE International Symposium on Industrial Electronics*, pp. 299–304, June 2018
48. Y. Liu, Y. Wang, S. Ding, Y. Tao, W. Li, A boost converter integrated with DC circuit breaker, in *IEEE Industrial Electronics Conference*, October 2021